



## Doubled single-frequency Nd:YLF ring laser coupled to a passive, non-resonant cavity

Yann Louyer, Patrick Juncar, Mark David Plimmer, Thomas Badr, François Balembois, Patrick Georges, Marc Himbert

### ► To cite this version:

Yann Louyer, Patrick Juncar, Mark David Plimmer, Thomas Badr, François Balembois, et al.. Doubled single-frequency Nd:YLF ring laser coupled to a passive, non-resonant cavity. *Applied optics*, 2004, 43 (8), pp.1773-1776. 10.1364/AO.43.001773 . hal-00700763

**HAL Id: hal-00700763**

**<https://hal-iogs.archives-ouvertes.fr/hal-00700763>**

Submitted on 23 May 2012

**HAL** is a multi-disciplinary open access archive for the deposit and dissemination of scientific research documents, whether they are published or not. The documents may come from teaching and research institutions in France or abroad, or from public or private research centers.

L'archive ouverte pluridisciplinaire **HAL**, est destinée au dépôt et à la diffusion de documents scientifiques de niveau recherche, publiés ou non, émanant des établissements d'enseignement et de recherche français ou étrangers, des laboratoires publics ou privés.

# Doubled single-frequency Nd:YLF ring laser coupled to a passive nonresonant cavity

Yann Louyer, Patrick Juncar, Mark D. Plimmer, Thomas Badr, François Balembois, Patrick Georges, and Marc E. Himbert

We demonstrate an original solution to obtain a single-frequency ring laser coupled to an external passive nonresonant ring cavity, which plays the role of an optical diode. This system provides more output power than systems with an intracavity unidirectional device. To the best of our knowledge, this work marks the first demonstration of a unidirectional planar ring laser at 1.3  $\mu\text{m}$ . Using 12 W at 797 nm to pump a Nd:YLF laser, combined with intracavity second-harmonic generation, we achieve yields of 440 mW at 661.3 nm and 340 mW at 656.0 nm. © 2004 Optical Society of America

OCIS codes: 140.3320, 140.3380, 140.3580, 140.3560, 140.3410, 140.3570.

## 1. Introduction

### A. Motivation

We develop an optical clock based on the narrow two-photon transition in Ag.<sup>1</sup> To observe the transition with an atomic beam requires  $\geq 500$  mW at 661.3 nm, whereas, for laser cooling,  $\geq 100$  mW at 328 nm is desirable.<sup>2</sup> Generating the latter by frequency doubling implies  $\geq 500$  mW at 656 nm.<sup>3</sup> To avoid using dye lasers, we build diode-pumped Nd<sup>3+</sup>-doped YLiF<sub>4</sub> lasers (hereafter Nd:YLF). We have already demonstrated standing-wave lasers with  $\leq 750$  mW single-mode power at 1.3  $\mu\text{m}$ .<sup>4,5</sup> Here we present a novel ring laser that provides greater single-frequency output and intracavity second-harmonic generation (SHG).

### B. Traditional Methods for Achieving Unidirectional Operation

Because they avoid spatial hole burning, traveling wave lasers generally provide greater output power and better frequency stability than do their standing-wave counterparts and show identical intracavity losses. The essential difference between the two is that there is a means of ensuring unidirectional operation in the latter method. Among the different techniques to achieve this, the most frequently employed is an intracavity Faraday rotator whose rotation for one sense of propagation is compensated by the rotation due to an optically active crystal.<sup>6</sup> Other solutions include using a nonplanar ring cavity<sup>7,8</sup> or acousto-optically induced feedback.<sup>9</sup> The nonplanar technique is inapplicable here because Nd:YLF is birefringent, while the low gain of the medium<sup>10</sup> rules out the latter technique. Thus we began with a conventional ring laser containing an optical diode. The unpolarized beam from a fibre diode pump (Limo Model HLU25F200; cooled to 6 °C to emit at 797 nm where Nd:YLF has an absorption line) is collimated and focused by two doublets to a waist of 280  $\mu\text{m}$  in the 0.7% Nd<sup>3+</sup>-doped YLF crystal ( $3 \times 3 \times 10$  mm<sup>3</sup>). Laser operation around 1312 or 1322.6 nm is selected by the orientation of the polarization relative to the *c* axis of the crystal<sup>10</sup> (perpendicular for 1312 nm, parallel for 1322.6 nm). Fine wavelength tuning is achieved by use of a solid 0.1-mm thick Suprasil etalon. All mirrors are highly reflecting at 1.3  $\mu\text{m}$  so as to maximize intracavity power for SHG. The optical diode consists of a Faraday rotator (FR<sub>1</sub>) made from terbium gallium

Y. Louyer, P. Juncar, M. D. Plimmer (mark.plimmer@cnam.fr), T. Badr, and M. E. Himbert are with the Bureau National de Métrologie—Institut National de Métrologie, Conservatoire National des Arts et Metiers, 292 rue Saint-Martin, Paris F75003, France. Y. Louyer, F. Balembois, and P. Georges are with the Laboratoire Charles Fabry, Institut d'Optique Théorique et Appliquée, Unité mixte du Centre National de la Recherche Scientifique et de l'Université de Paris-Sud, Centre Universitaire, Bât. 503, Orsay F91403, France.

Received 27 August 2003; revised manuscript received 25 November 2003; accepted 12 December 2003.

0003-6935/04/081773-04\$15.00/0

© 2004 Optical Society of America

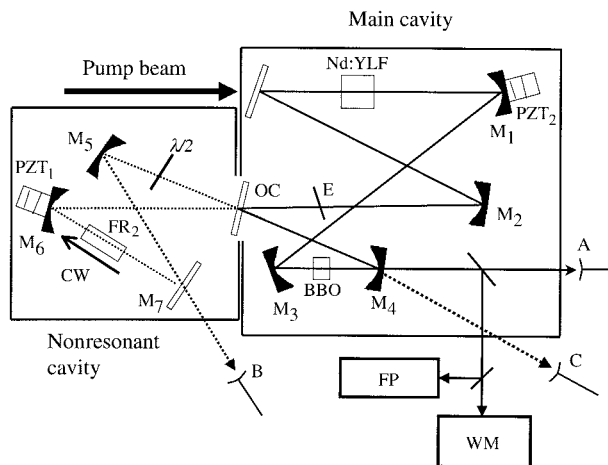


Fig. 1. Six-mirror cavity reinjected by use of a passive nonresonant cavity formed by  $M_5$ ,  $M_6$ , and  $M_7$  and the output coupler OC ( $T = 2\%$ ). All other mirrors have  $R_{\max}$  at  $1.3 \mu\text{m}$ . For SHG, a BBO crystal can be placed between  $M_3$  and  $M_4$ .  $FR_2$ ,  $50^\circ$  Faraday rotator; E, solid etalon (0.1 mm). Photodiodes A, main cavity clockwise power; B, external (clockwise); C, main (counterclockwise);  $PZT_1$  and  $PZT_2$ , piezoelectric transducers; FP, Fabry-Perot spectrum analyzer; WM, wavemeter;  $\lambda/2$ , half-wave plate.

garnet ( $\text{Te}_3\text{Ga}_5\text{O}_{12}$ , known as TGG), providing a  $4^\circ$  rotation and a half-wave plate ( $\lambda = \text{wavelength}$ ). Owing to absorption within the TGG crystal, even without the etalon losses, we obtained only 40 W intracavity power at  $1.3 \mu\text{m}$  with 12 W of absorbed pump power at 797 nm. The intracavity power was deduced from the leakage through a high reflector (80 mW) with a transmission coefficient  $T_{\text{HR}} = 0.002$ . Worse still, thermal absorption of 2% (0.8 W) by  $FR_{11}$  soon caused the TGG crystal to break.

## 2. Nonresonant External Ring Cavity

Our solution to the above problem was to use an external passive, nonresonant cavity (henceforth referred to as NRC) to house the optically active elements (Fig. 1), with the much-lower intra-passive-cavity power traversing the rotator  $FR_2$  to avoid thermal damage. The corresponding reduction of losses in the main cavity leads to greater power (a valuable asset for SHG). The main ring resonator is coupled to the NRC via a  $T = 2\%$  output coupler that is common to both cavities. The effective optical diode is composed of a half-wave plate, antireflection coated for 1322 nm, and a TGG Faraday rotator  $FR_2$  ( $T = 80\%$  at  $1.3 \mu\text{m}$ ) turning the linear polarization by  $50^\circ$ , both in the NRC, together with the birefringent laser crystal in the main cavity. The resulting losses in the main cavity (arising from the polarization tilt and the birefringence of the Nd:YLF crystal) are higher for the counterclockwise circulating beam than for the clockwise one, a difference sufficient to impose unidirectional laser operation in the clockwise sense. The use of the external cavity to influence laser performance is described elsewhere<sup>11–13</sup> and entails a single injecting external mirror used to increase one-way oscillation in a three-mirror ring

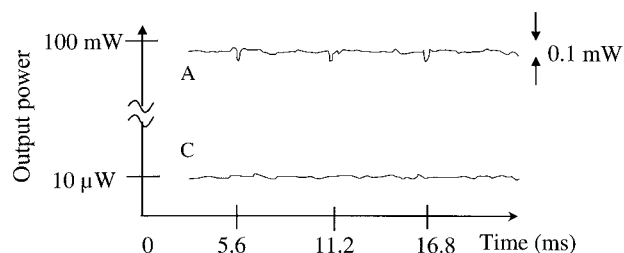


Fig. 2. Passive output powers from the main cavity as a function of time: A, clockwise; C, counterclockwise. The glitches at the 0.1% level are due to current instabilities in the pump diode power supply.

resonator. In those applications the goal was mode selection and not unidirectional operation. In fact, the quasi-unidirectional laser built in this way is susceptible to mode hops, which explains why we chose a different scheme. In our case, because we use an external ring cavity, the reinjected beam that drives the clockwise oscillation is the clockwise one; i.e. it rotates in the same sense. The laser wavelength is measured with a wavemeter (Burleigh WA-1000). The longitudinal mode of the ring laser (spacing 290 MHz) is analyzed with a 750-MHz free-spectral-range scanning confocal interferometer. Figure 2 shows that the signals are proportional to the power of the waves traveling in both directions, as recorded by the photodiodes. Note that the use of the NRC has no effect on the mode structure of the main cavity because the laser remains single frequency. This is evidenced by the fact that no mode hops were observed during several tens of seconds of free-running operation of the laser. Moreover, once the counterclockwise oscillation is nearly extinguished, a very robust unidirectional laser operation is obtained and lasts for hours. In this case the intracavity power (leakage  $210 \text{ mW}/T_{\text{HR}} = 0.002$ ) exceeds 100 W, i.e., is 2.5 times that obtained with a conventional ring resonator.

In general, critical alignment procedures are necessary with set ups that use an external resonant cavity scheme. This results in significant power and phase changes and requires servo electronics. In our case, however, internal and external beam powers show no strong interference effects when the NRC beam reinjects the ring laser because the external cavity mode structure does not match that of the main one. Thus the alignment accuracy of the mirrors of the NRC need not be interferometric. A key parameter here is the very weak coupling between the low-finesse NRC and the ring resonator. Only  $\approx 3 \times 10^{-4}$  of the ring laser intracavity power is reinjected into the ring cavity, which is sufficient to assure unidirectional operation. The observed variation of the total output power is only  $\approx 1\%$ . The laser beam phase is governed not only by the ring laser cavity length or electric field condition on the common mirror (either zero or a maximum) but also by the matching of the ring laser beam phase relative to that of the NRC. This effect can be seen in Fig. 3

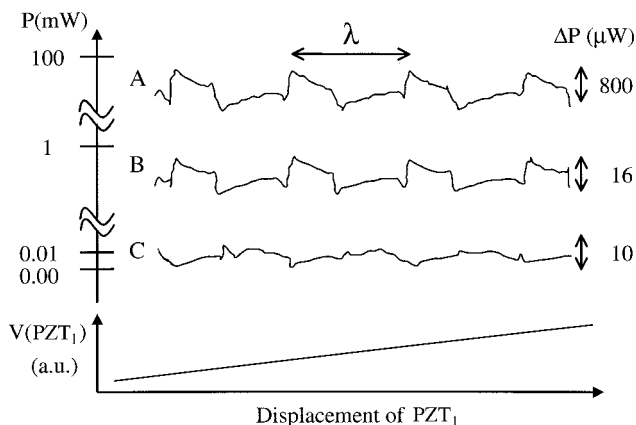


Fig. 3. Outputs from the main and reinjecting cavities as the length of the latter is varied using PZT: A, main (clockwise); B, reinjecting (clockwise); C, main (residual counterclockwise). Variations in A and B are due to polarization effects.<sup>14</sup> The glitches in C arise from pump diode power supply fluctuations.

in which the two signals A and B exhibit a weak periodic variation in phase as the mirror  $M_6$  of the NRC is displaced (Fig. 1). The small ac variation of the detected power (A, B) with a period of  $\lambda$  is evidence of the residual weak interaction between the phase-matched beams. Figure 3 shows the NRC wave traveling in the clockwise direction (B) and the waves in the ring laser traveling in both clockwise (A) and counterclockwise directions (C) as we scan the NRC length over a few wavelengths by using the piezoelectric transducer PZT<sub>1</sub>. The rather weak signal due to the counterclockwise beam (signal C) has the ac part of its phase shifted by  $\approx 180^\circ$  relative to the signals due to the clockwise beams (A and B). Moreover, this counterclockwise power is very small compared with that observed in the other external coupling scheme used to enhance clockwise operation; i.e., the one using a single external mirror.<sup>11,12,13</sup> In our case, because the counterclockwise beam circulating in the ring laser cavity has a power  $10^4$  times weaker than the clockwise one, the laser can be deemed unidirectional. For optimal performance one could always servo lock the laser output power close to its maximum value (i.e., the value that corresponds to the minimum counterclockwise power) and derive the required error signal from the two outputs A and C of Fig. 1.

### 3. Frequency Doubling

The reduction of losses in the main cavity leads to increased fundamental power, a great advantage for intracavity frequency doubling. To perform SHG, we insert between mirrors  $M_3$  and  $M_4$  a type-I  $\beta$ -BaB<sub>2</sub>O<sub>4</sub> frequency-doubling crystal, 7 mm long and with both faces antireflection coated at 1322 and 661 nm. The average spot size in the crystal is 45  $\mu$ m. With 12.0(2) W of absorbed pump power at 797 nm, the maximum output powers at 661.3, 656.0 and 660.5 nm (the gain maximum) are 440(10), 340(10), and 660(10) mW, respectively (see Fig. 4).

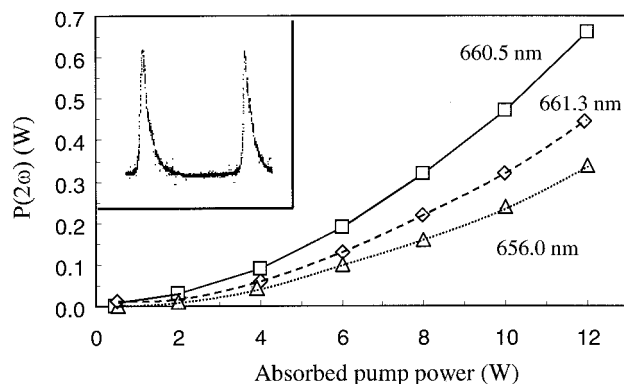


Fig. 4. SHG yields  $[P(2\omega)]$  versus pump power at  $\lambda_p = 797$  nm. Inset: Fabry-Perot transmission at  $1.322 \mu\text{m}$ , confirming single-mode generation of 661.3 nm.

By contrast, using a conventional ring laser with an intracavity TGG Faraday rotator, even without the losses of the solid etalon, we obtained only 90(10) mW at 660.5 nm under identical pumping conditions. Moreover, intracavity SHG enhances intensity and frequency stability, as explained elsewhere.<sup>15</sup> To check the continuity of single-frequency operation as the wavelength is scanned, we vary the ring laser cavity length by a few micrometers (corresponding to 2.5 GHz) by ramping the voltage on PZT<sub>2</sub>.

### 4. Conclusion

We have presented a diode-pumped unidirectional Nd:YLF ring laser coupled to a nonresonant ring cavity. This novel system yields a higher intracavity power at a wavelength of  $1.3 \mu\text{m}$  than does a conventional ring laser containing a TGG optical diode under identical pumping conditions. Most important, the intensity instabilities from the external nonresonant cavity have no discernable effect upon the laser frequency, at once making the device a useable, practical tool. Nevertheless, the dynamic intensity and phase behavior of these configuration lasers merit further investigation.

Y. Louyer thanks the Ministère de la Jeunesse, de l'Éducation Nationale et de la Recherche for a research studentship. The authors are grateful to J. Guéna for critical reading of the manuscript.

### References

1. P. L. Bender, J. L. Hall, R. H. Garstang, F. M. J. Pichanick, W. W. Smith, R. L. Barger, and J. B. West, "Candidates for two-photon optical frequency standards," *Bull. Am. Phys. Soc.* **21**, 599 (1976).
2. G. Uhlenberg, J. Dirscherl, and H. Walther, "Magneto-optical trapping of silver atoms," *Phys. Rev. A* **62**, 0634041–0634044 (2000).
3. S. A. Burrows, S. Guérandel, E. A. Hinds, F. Lison, and M. G. Boshier, "Progress towards a precise measurement of the  $\text{He}^+$  2S Lamb shift," in *The Hydrogen Atom: Precision Physics of Simple Atomic Systems*, S. G. Karshenboim, F. S. Pavone, G. F. Bassani, M. Inguscio, and T. W. Hänsch, eds. (Springer-Verlag, Berlin, 2001), pp. 303–313.
4. Y. Louyer, F. Balembois, M. D. Plimmer, T. Badr, P. Georges,

- P. Juncar, and M. E. Himbert, "Efficient cw operation of diode-pumped Nd:YLF lasers at 1312.0 and 1322.6 nm for a silver atom optical clock," *Opt. Commun.* **217**, 357–362 (2003).
5. Y. Louyer, F. Balembois, M. D. Plimmer, P. Georges, P. Juncar, and M. E. Himbert, "Nd:YLF laser at 1.3  $\mu\text{m}$  for calcium atom optical clocks and precision spectroscopy of hydrogenic systems," *Appl. Opt.* **42**, 4867–4870 (2003).
  6. T. F. Johnston, Jr., R. H. Brady, and W. Proffitt, "Powerful single-frequency ring dye laser spanning the visible spectrum," *Appl. Opt.* **21**, 2307–2316 (1982).
  7. F. Biraben, "Efficacité des systèmes unidirectionnels utilisables dans les lasers en anneau," *Opt. Commun.* **29**, 353–356 (1979).
  8. T. J. Kane and R. L. Byer, "Monolithic, unidirectional, single-frequency mode Nd:YAG ring laser," *Opt. Lett.* **10**, 65–67 (1985).
  9. W. A. Clarkson and D. C. Hanna, "Acousto-optically induced unidirectional single mode operation of a Q-switched Nd:YAG ring laser," *Opt. Commun.* **81**, 375–378 (1991).
  10. L. Fornasiero, T. Kellner, S. Kück, J. P. Meyn, P. E.-A. Möbert, and G. Huber, "Excited state absorption and stimulated emission of  $\text{Nd}^{3+}$  in crystals III:  $\text{LaSc}_3(\text{BO}_3)_4$ ,  $\text{CaWO}_4$  and  $\text{YLiF}_4$ ," *Appl. Phys. B* **68**, 67–72 (1999).
  11. A. E. Siegman, *Lasers* (University Science, Mill Valley, Calif., 1986), p. 534.
  12. A. E. Siegman, "An antiresonant ring interferometer for coupled laser cavities, laser output coupling, mode locking and cavity dumping," *IEEE J. Quantum Electron.* **9**, 247–250 (1973).
  13. P. W. Smith, "Mode selection in lasers," *Proc. IEEE* **60**, 422–440 (1972).
  14. T. W. Hänsch and B. Couillaud, "Laser frequency stabilization by polarization spectroscopy of a reflecting reference cavity," *Opt. Commun.* **35**, 441–444 (1980).
  15. K. I. Martin, A. Clarkson, and D. C. Hanna, "Self-suppression of axial mode hopping by intracavity second-harmonic generation," *Opt. Lett.* **22**, 375–377 (1997).